| | |
|---|---|
| **Title** | Rare earth (La, Nd, Pr) doped ceria zirconia solid solutions for soot combustion |
| **Authors(s)** | Dulgheru, Petrica, Sullivan, James A. |
| **Publication date** | 2013-05 |
| **Publication information** | Dulgheru, Petrica, and James A. Sullivan. “Rare Earth (La, Nd, Pr) Doped Ceria Zirconia Solid Solutions for Soot Combustion.” Springer, May 2013. https://doi.org/10.1007/s11244-013-0006-5. |
| **Publisher** | Springer |
| **Item record/more information** | http://hdl.handle.net/10197/4256 |
| **Publisher's statement** | The final publication is available at www.springerlink.com |
| **Publisher's version (DOI)** | 10.1007/s11244-013-0006-5 |

# Rare Earth (La, Nd, Pr) Doped Ceria Zirconia Solid Solutions for Soot Combustion

P. Dulgheru*, J. A. Sullivan

UCD School of Chemistry and Chemical Biology, Belfield, Dublin 4, Ireland
* Faculte´ des Sciences, CPMCT Universite´ Libre de Bruxelles, Campus Plaine CP 243, 1050 Brussels, Belgium

## Abstract

A series of rare earth (RE) (La, Nd, Pr) ceria zirconia materials were analysed for their soot combustion activity in air and in NO/$O_2$. The materials were characterised using DRIFT spectroscopy. In general the presence of the RE dopant increases the activity of undoped $Ce_xZr_{1-x}O_2$. The La and Pr doped catalysts showed increased low temperature activity in the presence of NO/$O_2$ while the effect was less pronounced in case of Nd – doped samples. FTIR data has shown that the catalysts interact differently to NO/$O_2$ mixtures in that they do not form significant quantities of adsorbed nitrite-type species. We postulate that this species is a precursor to $NO_2$ formation which in turn increases soot combustion.

**Keywords** Lean burn _ Rare earth oxides _ Soot _Particulate matter _ Diesel engines _ Soot oxidation _DRIFTS spectroscopy _ TGA

## 1 Introduction

Diesel lean burn engines are more fuel efficient than gasoline engines. Their biggest disadvantage is that they emit carbonaceous particulate matter (PM) also called soot, a pollutant recently regulated by EU and US environmental legislation.

Currently all diesel vehicles Euro four compliant (i.e. registered later than 2005) are fitted with diesel particulate filters (DPF) which collect soot with efficiencies higher than 95 % [1, 2]. Although this filtration efficiency might seem high, certain researchers are concerned that current DPFs completely fail to filter very small particles (<2.5 μm) which pose a serious threat to human health [3].

Ideally, trapped soot is oxidised during high temperatures met while driving on the highway, when the exhaust temperature is sufficient for un-catalysed PM oxidation (500 °C). If the driver uses the car only for short urban trips DPF regeneration will not occur and the on-board diagnostic will inform the driver that the car needs to be serviced, where the DPF will either be replaced or manually cleaned.

In order to avoid problems related to uncontrolled DPF regeneration (DPF damage, engine damage, etc.) DPF manufacturers have introduced various ways to either increase exhaust temperatures (using post combustion injection of fuel, burners, electric heating the DPF) or decrease soot oxidation temperature using catalysts. Some manufacturers have opted for catalysed DPFs whose walls are coated with a layer of catalytic material (usually a ceria based oxide) which decreases the PM oxidation temperature to ~370 °C (which can be achieved more easily during urban and extra-urban driving).

$CeO_2$, previously used for its oxygen storage capacity in buffering three way catalysts against excursions from stoichiometric combustion, has been proposed as a promising soot oxidation catalyst to accelerate the soot - $O_2$ reaction. It has been reported that the gas-phase $O_2$ can replace $CeO_2$ lattice oxygen resulting in highly labile surface oxygen, which is able to react with soot. [4].

However, due to the tendency of $CeO_2$ to deactivate at high temperatures (through sintering), pure $CeO_2$ cannot be used in this application, and there is a need for thermally stable materials (i.e. those which can withstand temperatures up to 900 °C which can be reached during regeneration) [5].

One approach previously used to stabilize $CeO_2$ against sintering was to dope it with rare earth elements ($La^{3+}$, $Pr^{3+/4+}$, $Gd^{3+}$, $Nd^{3+}$) or transition metals (Fe, Y, Zr). [6–9] These efforts have shown that doping $CeO_2$ with certain rare earth and transition metal cations, not only produced materials with increased thermal stability, but in certain cases the doped samples also exhibited increased oxygen storage capacity. In the case of Zr-doped $CeO_2$ this beneficial effect is thought to be related to the creation of oxygen vacancies due to partial substitution of $Ce^{4+}$ ions (ionic radii = 0.97 Å ) with $Zr^{4+}$ ions (ionic radii = 0.84 Å). Given that the OSC is related to the potential concentration of vacancies, and given that the concentration of vacancies is related to the ‘‘active oxygen’’ discussed above, it is reasonable to assume that these materials will also act as improved combustion catalysts.

Oxygen vacancies are point defects in the $CeO_2$ lattice structure that are important in $CeO_2$ oxygen storage capacity, redox potential, and oxygen mobility. Oxygen vacancies can be generated by:

i. Introducing an isovalent but bulkier cation, which will produce a lattice expansion and will generate defects in the structure (e.g., some M–O bonds will break) [10].
ii. Reducing the sample, (generating $Ce^{3+}$ ions) forces the system to create oxygen vacancies (in order to maintain charge neutrality) [11, 12].

Due to its fluorite structure, the oxygen atoms in a $CeO_2$ crystal are all co-planar, allowing for rapid oxygen atom diffusion through the lattice as a function of the number of oxygen vacancies. As the concentration of vacancies increases, the ease at which oxygen can move around in the crystal increases, allowing the cerium cations to reduce and oxidize quite easily. Increasing the oxygen mobility, and implicitly [oxygen vacancies] is important in a series of applications including automotive exhaust after-treatment (the three way catalyst mentioned above), sensor applications (where electronic and $O^{2-}$ conductivity are important), water–gas shift catalysis and many others. [13–15].

Since the mobility of oxygen atoms is a critical property for most of the applications of these materials, and both isovalent and aliovalent doping increase this effect, more and more research groups have focused on doping $CeO_2$ with $Zr^{4+}$, $Pr^{3+/4+}$, $Nd^{3+}$, $La^{3+}$ and other rare earth oxides) [16–23]. In the $Ce_xZr_{1-x}O_2$ ($0<x<1$) solid solutions, cerium is the redox active while zirconium is the redox inactive component. It is quite obvious that introducing new ions in the $Ce_xZr_{1-x}O_2$ matrix will have an effect on the catalytic properties of these materials by either enhancing/diminishing the redox properties of the material or by improving/ damaging its textural properties.

The research put forth in this investigation is directed at understanding the extent to which further doping $Ce_xZr_{1-x}O_2$ with isovalent or aliovalent rare earth dopants can further increase the catalytic activity of these materials in oxidation of carbonaceous PM using $O_2$ or $NO/O_2$.

## 2 Experimental

### 2.1 Catalyst Preparation and Catalyst Soot Mixtures

Solid solutions of ceria zirconia and rare earth doped ceria zirconia materials were prepared by MEL chemicals using a proprietary method (Table 1). The prepared materials consisted of a series of ceria zirconia rare earth oxide doped materials having the following formula: $Ce_{0.3}RE_{0.2}Zr_{0.5}O_2$ (RE = Nd, La, Pr) and a subfamily of materials containing various loadings of Praseodymium 5, 15 and 20 % Praseodymium doped ceria zirconia.

The soot surrogate used in this work was industrial flame soot manufactured by Degussa AG (Printex-U) which simulates the properties of real diesel soot [24]. Catalyst materials were mixed with soot in a 50:1 catalyst to soot ratio (by mass). The catalyst/soot mixtures were mixed for 5 min in a glass vial using a spatula. This yields a loose contact situation. The mixture was then wet with methanol until a paste was formed and dried for 2 h at 70 °C.

Table 1 notations and composition of samples prepared by MEL chemicals

| | $Ce_{0.3}La_{0.2}Zr_{0.5}O_2$ | $Ce_{0.3}Nd_{0.2}Zr_{0.5}O_2$ | $Ce_{0.3}Pr_{0.2}Zr_{0.5}O_2$ | $Ce_{0.3}Pr_{0.15}Zr_{0.5}O_2$ | $Ce_{0.3}Pr_{0.05}Zr_{0.5}O_2$ |
|---|---|---|---|---|---|
| Notation | CeZLa20 | CeZNd20 | CeZPr20 | CeZPr15 | CeZPr05 |
| + Printex U (50:1) | CeZLa20-U | CeZNd20-U | CeZPr20-U | CeZPr15-U | CeZPr05-U |
| BET ($m^2$ $g^{-1}$) | 69 | 49 | 95 | 69 | 110 |

## 2.2 Catalyst Characterisation

### 2.2.1 Thermogravimetric Analysis

Thermogravimetric analysis was carried out using a Q500 TGA (TA Instruments) thermogravimetric balance equipped with an Evolved Gas Analysis (EGA) furnace. The EGA furnace was fitted with an exhaust port which allowed coupling of the TGA to a Quadrupole MS (HPR20, Hiden). This tandem TGA-MS system was able to monitor both the mass loss (both as TGA and DTGA profiles) and the composition of desorbed gases simultaneously. The catalyst soot mixtures were held in a flow of air or $NO/O_2$ (90 mL $min^{-1}$) and the temperature was ramped at a rate of 10 °C $min^{-1}$ to 800 °C.

### 2.2.2 Surface Area Measurements

The materials were characterised by MEL Chemicals using a NovaWin220 (Quantachrome Instruments) BET analyser. Surface area was determined using multipoint $N_2$ adsorption at -196 °C and was calculated from the linear part of the BET plot.

## 2.3 Drifts

Infrared spectra (4 $cm^{-1}$, 256 scans, Kubelka–Munk units) were recorded using a Vertex 70 (Bruker) equipped with an MCT detector (operated at -196 °C). In situ diffuse reflectance spectra were carried out in a specially designed catalytic cell (HVC-DRP-4, Harrick) which was placed inside the Praying Mantis (Harrick Sci.) diffuse reflectance accessory. In situ experiments were carried out isothermally at 400 °C in a flow of 2,000 ppm NO and 10 % $O_2$ over the materials in the presence and absence of Printex U.

## 4 Results and Discussions

Figure 1 shows the derivative weight change profiles (displaced) recorded during exposure of rare earth doped samples mixed with Printex U and exposed to air (upper panel) or 2,000 ppm NO and 10 %$O_2$ (lower panel). All samples were able to initiate soot oxidation at temperatures below 400 °C, with slightly lower temperatures in the presence of NO/$O_2$ compared to similar experiments carried out in air. As a general rule, in the presence of NO/$O_2$, $T_{ini}$ was ~100 °C lower compared to similar experiments carried out in air.

.

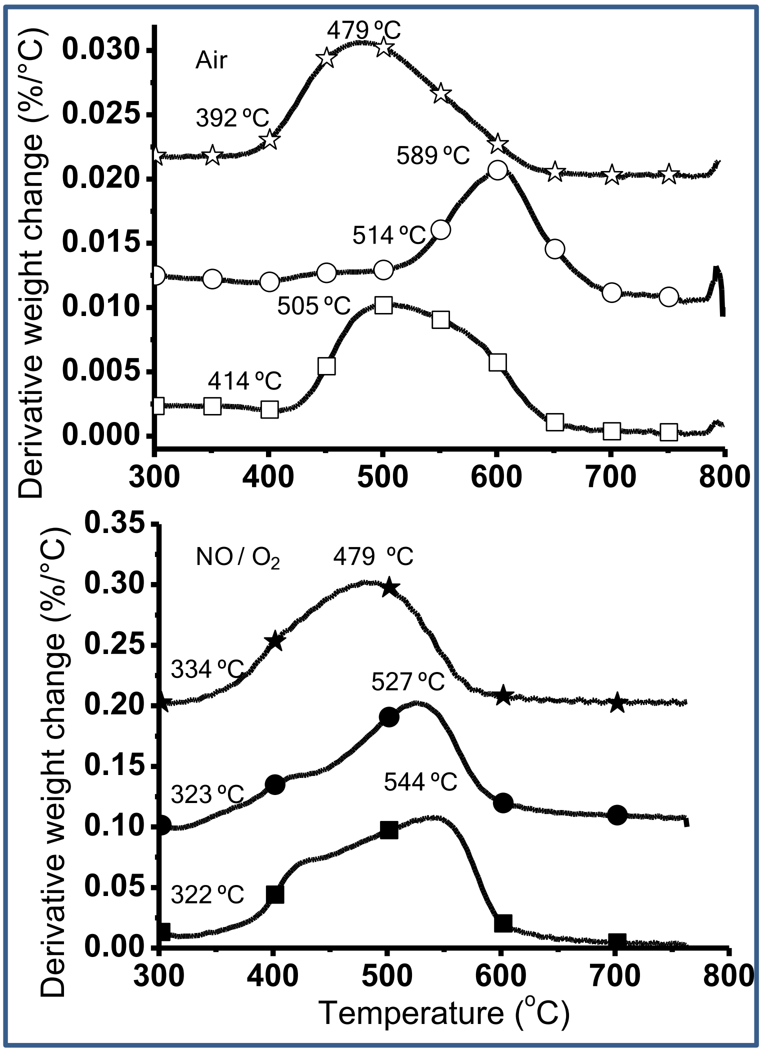

Figure 1 Derivative weight change profiles recorded during exposure of rare earth doped samples mixed with Printex U in 50:1 ratio and exposed to air (upper panel, empty symbols) and $NO/O_2$ (lower panel, full symbols) while being heated from RT – 800 °C (with a 10 °C min-1 ramp rate). CeZLa20–U (☆,★), CeZPr20–U (○,●) CeZNd20-U (□,■). Profiles were displaced for clarity.

CeZLa20 sample was the most active material in Printex U oxidation reaction with Tmax of ~480 °C in both air and $NO/O_2$. This $T_{max}$ is inferior to similar results recorded during experiments carried out on $CeO_2$ and $Ce_xZr_{1-x}O_2$ materials calcined in identical conditions (experiments not shown). Similar results have been previously observed by other researchers [8, 20, 25, 26] which have correlated the increased activity of lanthanum doped ceria samples to preservation of textural properties during high temperature treatment (i.e. pure $CeO_2$ samples aged at 850 °C lost 50 % of their surface area while lanthanum doped were virtually unaffected).

Surprisingly, CeZPr20 sample oxidised Printex U in air at a $T_{max}$ of ~590 °C, the temperature being slightly inferior to the un-catalysed process. A slightly lower oxidation temperature was recorded when exposing CeZPr20-U to NO and $O_2$ (i.e. 525 °C).

This result was disappointing in the light of work published by to Bakhmutsky et al. [27] who suggested that praseodymium can shift its oxidation state from 4+ to 3+ (in a similar manner to cerium). This implicitly suggested that preparing a material with both $Ce^{4+/3+}$ and $Pr^{4+/3+}$ ions should result in a material with increased oxygen mobility which should make it an extremely good material in oxidising reactions. This was not the case with CeZrPr20 material which commenced Printex U oxidation in air at a slightly lower temperature compared to non-catalysed experiments in air. Although there is a slight promotional effect, the CeZPr20 sample was far from being the most efficient material. CeZNd20 sample slightly decreased Printex U oxidation temperature but was still not as active compared to the CeZLa20 sample in both air and $NO/O_2$. This might be directly connected to the fact that the neodymium doped sample had a lower surface area than the other two catalysts (i.e. 49 $m^2g^{-1}$ (CeZNd20) vs. 69 $m^2g^{-1}$ (CeZLa20) vs. 95 $m^2g^{-1}$ (CeZPr20)). This in turn suggests that neodymium was less effective at stabilising the $CeO_2$ surface during the high temperature calcination.

Surprisingly, in case of the neodymium containing sample, although soot oxidation commenced at a lower temperature in the presence of $NO/O_2$ (414 °C in air vs 322 °C in $NO/O_2$) the maximum rate of soot combustion was negatively affected by the presence of $NO/O_2$ (505 °C versus 544 °C).

### 4.1 Effect of Praseodymium Concentration upon Soot Oxidation

Figure 2 shows the derivative weight change (%/ °C) profiles from CeZPr(5–20)–U samples in the presence of 2,000 ppm NO and 10 % $O_2$ (lower panel) or air (upper panel) while being heated from RT – 800 °C. As previously observed, maximum Printex U oxidation using NO/$O_2$ takes place at slightly lower temperatures with differences (i.e. vs. experiments in air) observed in $T_{max}$ ranging from 55 °C (5 %Pr) and 85 °C (20 %Pr). The combustion activity increases as the [Pr] within the catalyst is increased at the expense of the [Zr]. Irrespective of the [Pr] the materials are not especially good catalysts for the combustion of Printex U (note $T_{max}$ is slightly below the temperature region where graphite combustion takes place).

A far higher difference is observed when taking into account the temperature at which soot oxidation commences. For example, Printex U starts oxidising at ~320 °C (CeZPr20 in NO/$O_2$) while in air, these materials start oxidising soot at 450 °C (see filled star and empty star profiles in Fig. 2). It is not unlikely that in presence of NO/$O_2$ soot is oxidised via two different mechanisms. At temperatures of around 300 °C it could be possible that the CeZPr20 sample catalyses the oxidation of NO to $NO_2$ which could then go on and commence soot oxidation. At higher temperatures, the production of $NO_2$ is unfavoured, soot oxidation could continue via mobile oxygen species given-off by $Pr^{4+/3+}$ and $Ce^{4+/3+}$.

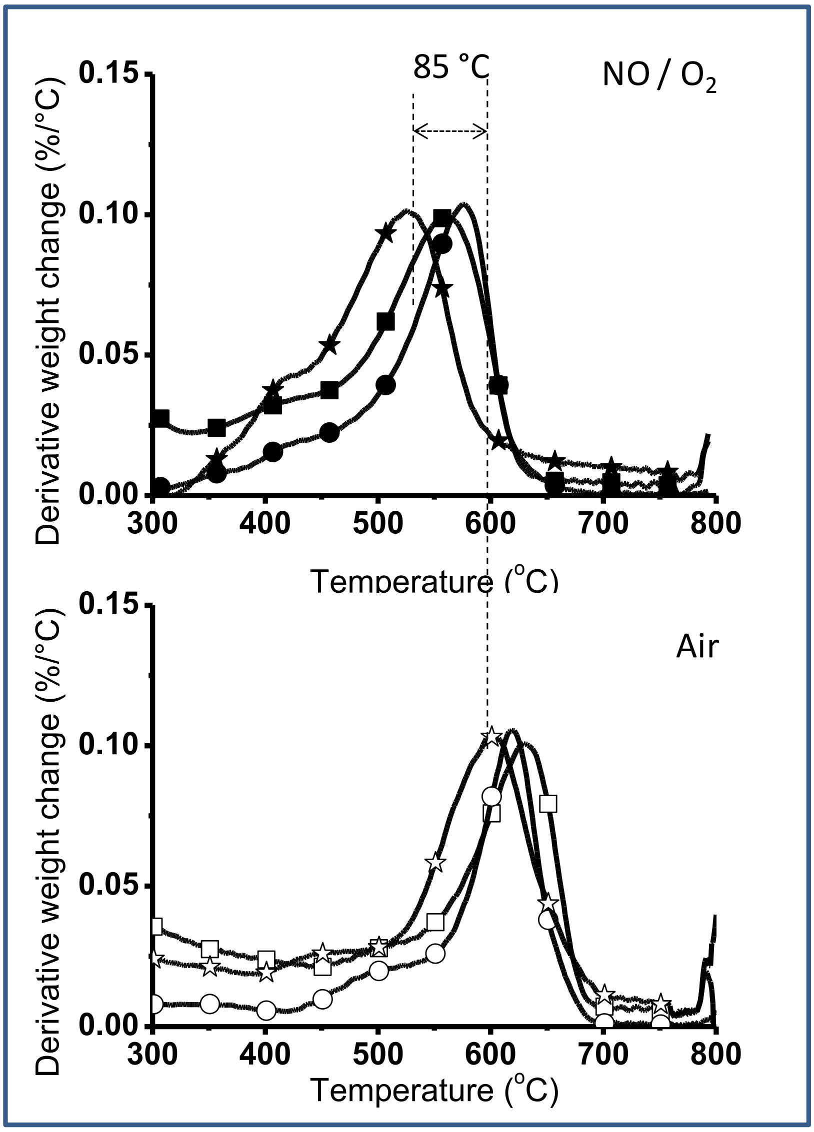

Figure 2 Derivative weight change ( % / °C) signal recorded by the TGA during exposure of $Ce_{0.3}Pr_{0.05-02}Zr_{0.65-0.5}O_2$ – U to either 2000 ppm NO and 10% $O_2$ (at 400 °C) (upper panel, full symbols) or air (lower panel, empty symbols). $Ce_{0.3}Pr_{0.2}Zr_{0.5}O_2$ (★,☆) $Ce_{0.3}Pr_{0.15}Zr_{0.5}O_2$ (●,○) $Ce_{0.3}Pr_{0.05}Zr_{0.5}O_2$ (■,□).

## 4.2 In Situ Drifts

In situ DRIFTS experiments carried out over fresh rare earth ceria zirconia samples exposed to a flow of 2,000 ppm NO and 10 % $O_2$ at 400 °C, resulted in the appearance of 2 strong bands (at 1,560 and 1,300 $cm^{-1}$). Another weaker, less intense band was also observed at approximately 1,050 $cm^{-1}$ for CeZLa20 and CeZPr20 (see Fig. 3, panels A and C). This band is exceptionally weak for the

CeZNd20 sample. These bands have been previously observed during NO/O$_2$ studies over oxide surfaces (on platinum-based catalysts) and their presence has been attributed to the formation of bulk nitrate species (1,560 cm$^{-1}$ band), surface nitrites (1,300 cm$^{-1}$) and adsorbed nitrite species (1,050 cm$^{-1}$) (see Fig. 3).

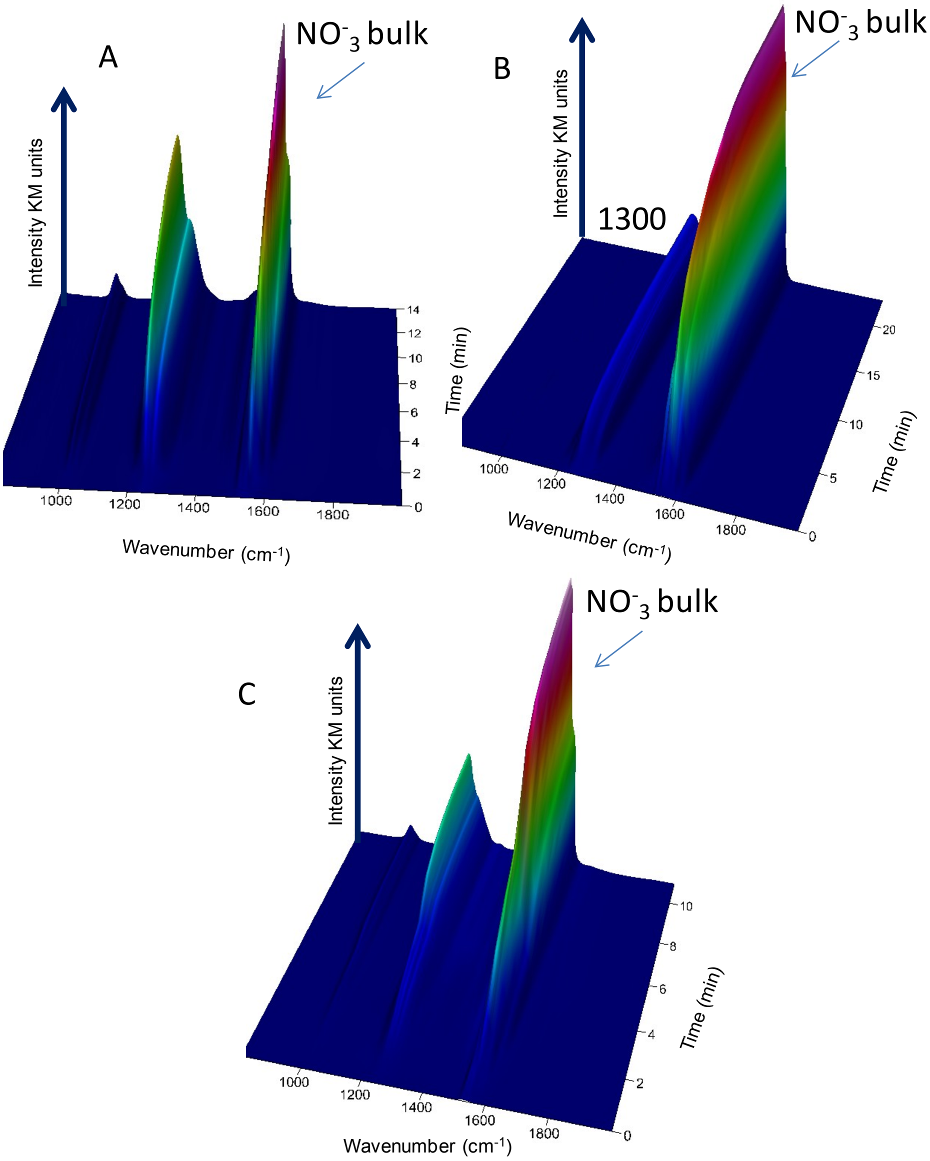

Figure 3 in situ DRIFT spectra recorded during exposure of CeZLa20 (A) , CeZNd20 and CeZPr20 to 2000 ppm of NO and 10% O$_2$ at 400 °C. Spectra were recorded for periods of time ranging from 10 to 20 minutes. Besides the vibration which can be assigned to nitrate species formed on the surface, the rest have been omitted for clarity of the figure. For more information see text.

It is widely accepted in the literature that the formation of nitrate species over oxide materials is usually observed when samples are exposed to $NO_2$ flue (and only following extended exposure times and in presence of a noble metal if NO rather than $NO_2$ is present). In our experiments CeZLa20, CeZPr20 and CeZNd20 materials were exposed to a flow of NO and $O_2$ (at 400 °C) in the absence of a noble metal component. The formation of bulk nitrates suggests that these samples might be able to oxidise NO to $NO_2$. This is not very difficult to believe as these materials have known oxygen storage/oxygen release properties. If this would be the case, then Printex U oxidation activity in $NO/O_2$ presented in Fig. 1 and Fig. 2 could be explained by the ability of these materials to generate a combination of nitrite/nitrate adsorbed and $NO_2$ gaseous species (in the 200–400 °C range) which can then be used to oxidise Printex U.

In order to test this theory we exposed a CeZLa20-U sample to a flow of 2,000 ppm NO and 10 % $O_2$ at 400 °C while monitoring the reaction using in situ DRIFT spectroscopy for about 20 min (see Fig. 4). Although at the start of the experiment, the mixture looked dark black after about 15 min in the reaction conditions grey spots were easy to notice suggesting Printex U was oxidised and had partially disappeared from the reactor.

Figure 4 shows the 800 – 1,700 $cm^{-1}$ region of the IR spectrum recorded during exposure of the CeZLa20-U sample to a flow of $NO/O_2$ at 400 °C. Three vibrational bands which we assigned to C–O vibrations (1,000 – 1,100 $cm^{-1}$) C–$NO_2$ (1,250–1,400 $cm^{-1}$) and C = O (1,500–1,600 $cm^{-1}$) are clearly observed as soon as the

$NO/O_2$ is introduced in the reactor. Because of the sample colour, the experiment could not be run in absorbance or transmittance mode and we had to perform the experiment in Kubleka-Munk (KM) mode, which in turn did not allow us to monitor Printex U disappearance (all peaks are positive in KM). It is worth mentioning though, that assigning any particular vibration in this region of the spectrum is fraught as several overlapping vibration modes are possible.

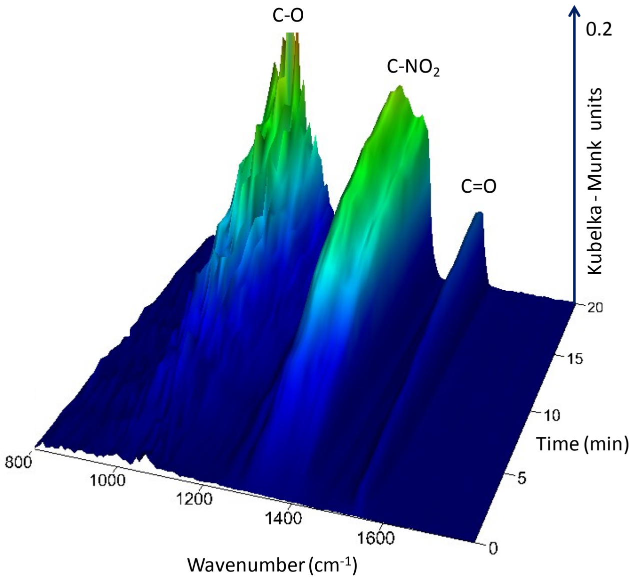

Figure 4 showing the 800-1800 cm$^{-1}$ region of the IR spectrum recorded during exposure of a CeZLa20-U sample exposed 2000 ppm NO and 10%$O_2$ at 400 °C. A background spectrum was recorded at the start of the experiment (before $NO/O_2$ mixture was admitted in the reaction chamber).

## 5 Conclusions

Printex U oxidation using a series of high temperature composite materials having the following formula: $Ce_{0.3}RE_{0.2}Zr_{0.5}O_2$ (RE = $La^{3+}$, $Pr^{4+/3+}$, $Nd^{3+}$). These materials were prepared by MEL Chemicals. $Ce_{0.3}La_{0.2}Zr_{0.5}O_2$ was found to be the most active material of the group studied (it decreased Printex U oxidation temperature by ~200

°C in both air and $NO/O_2$). This increased activity was explained by an improved stabilisation of the textural properties of $CeO_2$ in the presence of La compared to the stabilizations seen in the presence of Nd and Pr.

While the initial temperature of combustion over this catalyst was decreased by the addition of $NO/O_2$, the maximum temperature of combustion of Printex U oxidation was not further promoted by exposing the $Ce_{0.3}La_{0.2}Zr_{0.5}O_2$ catalyst to $NO/O_2$. On the other hand, Printex U oxidation in the presence of $Ce_{0.3}Nd_{0.2}Zr_{0.5}O_2$ was reduced only slightly (~50 °C) when the catalyst soot mixture was exposed to $NO/O_2$.

This result, along with the absence of DRIFT peaks relating to adsorbed nitrite species (precursors to surface nitrite and $NO_2$ formation) was correlated to the lower surface area of this material (49 $m^2$ $g^{-1}$) compared to the surface area of the lanthanum containing sample (69 $m^2$ $g^{-1}$). The decreased activity may also be related to the oxygen transport properties.

Surprisingly, exposing $Ce_{0.3}Nd_{0.2}Zr_{0.5}O_2$ mixed with Printex U to $NO/O_2$ resulted in a higher temperature needed to reach the maximum rate of Printex U oxidation (again suggesting the catalysts was not active in the NO to $NO_2$ reaction) unlike $Ce_{0.3}RE_{0.2}Zr_{0.5}O_2$ (RE = $La^{3+}$, $Pr^{4+/3+}$).

The Praseodymium doped sample was also active in Printex U oxidation. This activity was further increased in $NO/O_2$. Increasing the concentration of praseodymium at the expense of zirconium results in materials more active in Printex U oxidation.

DRIFT experiments have confirmed the existence of various vibrations which could be attributed to nitrate/ nitrate species which are known to be the caused by $NO_2$, suggesting these materials are active in $NO_2$ oxidation (most likely via a Mars Van Krevelen mechanism). The ability of these materials to generate $NO_2$ species could therefore be responsible for their increased activity in Printex U oxidation.

## Acknowledgments

The authors would like to thank MEL Chemicals for providing the $CeZrO_2$ and $CeREZrO_2$ rare earth doped materials, and especially Mila Bortun from MEL Chemicals Inc. (USA) for preparing the RE doped Ce/Zr materials, Debra Harris from MEL Chemicals Inc. (UK) for and BET data, and also Heather Bradshaw for fruitful discussions. We would also want to thank the Environmental Protection Agency for funding the project under the STRIVE program as well as Roberto Rocca Educational Program for awarding PD one of their fellowships.

## References

1. Shah SD, Cocker DR, Johnson KC, Lee JM, Soriano BL, Miller JW (2007) Environ Sci Technol 41:5070
2. Ntziachristos L, Samaras Z, Zervas E, Dorlhene P (2005) Atmos Environ 39:4925
3. Lonati G, Ozgen S, Giugliano M (2007) Atmos Environ 41:4599
4. Bueno-Lopez A, Krishna K, Makkee M, Moulijn J (2005) Catal Lett 99:203
5. Balducci G, Fornasiero P, Dimonte R, Kaspar J, Meriani S, Graziani M (1995) Catal Lett 33:193
6. Loong CK, Ozawa M (2000) J Alloy Compd 303:60

7. Hu YC, Yin P, Liang T, Jiang W, Liu B (2006) J Rare Earths 24:86

8. Krishna K, Bueno-Lopez A, Makkee M, Moulijn JA (2007) Appl Catal B 75:189

9. Sha XQ, Lu Z, Huang XQ, Miao JP, Ding ZH, Xin XS, Su WH (2007) J Alloy Compd 428:59

10. Chen C-Y, Chang K-H Sens Actuators B 162:68

11. Suresh B, Ranjith T, Talgat I, Richard D, Alfons S, Sudipta S (2009) Nanotechnology 20:085713

12. Yang Z, Luo G, Lu Z, Woo TK, Hermansson K (2008) J Phys: Condens Matter 20:035210

13. Gonzalez-Velasco JR, Gutierrez-Ortiz MA, Marc JL, Gonzalez-Marcos MP, Blanchard G (2001) Appl Catal B 33:303

14. Craciun R, Daniell W, Knozinger H (2002) Appl Catal A 230:153

15. Fu Q, Kudriavtseva S, Saltsburg H, Flytzani-Stephanopoulos M (2003) Chem Eng J 93:41

16. Rossignol S, Descorme C, Kappenstein C, Duprez D (2001) J Mater Chem 11:2587

17. Rossignol S, Descorme C, Kappenstein C, Duprez D (2002) Scientific Bases for the Preparation of Heterogeneous Catalysts, vol 143, p 601

18. Torrens R, Sammes NM, Tompsett G (2004) J Electroceram 13:683

19. Ji Y, Liu J, He TM, Wang JX, Su WH (2005) J Alloy Compd 389:317

20. Krishna K, Bueno-Lopez A, Makkee M, Moulijn JA (2007) Appl Catal B 75:210

21. Fornasiero P, Balducci G, DiMonte R, Kaspar J, Sergo V, Gubitosa G, Ferrero A, Graziani M (1996) J Catal 164:173

22. Gogotsi GA (1997) Refract Ind Ceram 38:224

23. Trovarelli A, Zamar F, Llorca J, deLeitenburg C, Dolcetti G, Kiss JT (1997) J Catal 169:490

24. Saab E, Aouad S, Abi-Aad E, Bokova M, Zhilinskaya E, Aboukaıs A (2007) Kinet Catal 48:841

25. Krishna K, Bueno-Lopez A, Makkee M, Moulijn JA (2007) Appl Catal B 75:201

26. Krishna K, Bueno-Lopez A, Makkee M, Moulijn JA (2007) Top Catal 42–43:221

27. Bakhmutsky K, Zhou G, Timothy S, Gorte RJ (2009) Catal Lett 129:61